Fabrication and Electrokinetic Motion of Electrically Anisotropic Janus Droplets in Microchannels

Mengqi Li and Dongqing Li*

Department of Mechanical and Mechatronics Engineering, University of Waterloo, Waterloo, Ontario, Canada N2L 3G1

*Corresponding author, Address: 200 University Ave. West, Waterloo, Ontario, N2L 3G1

Email: dongqing@uwaterloo.ca (D. Li)

Statement

This is the peer reviewed version of the following article: Li, M. and Li, D. (2017), Fabrication and electrokinetic motion of electrically anisotropic Janus droplets in microchannels. ELECTROPHORESIS, 38: 287–295. doi:10.1002/elps.201600310, which has been published in final form at http://dx.doi.org/10.1002/elps.201600310. This article may be used for non-commercial purposes in accordance with Wiley Terms and Conditions for Self-Archiving.

Abstract

This paper presents experimental investigations of the fabrication and the motion of electrically anisotropic Janus droplets in a microchannel under externally applied direct current (DC) electrical field. The fabrication method of the Janus droplets is presented first. To begin, oil droplets are coated uniformly with positively charged nanoparticles in the aluminum oxide nanoparticle suspension. The electrically anisotropic Janus droplets are formed when the nanoparticles are accumulated to one side of the droplets in response to externally applied direct-current electric field. The surface coverage of the Janus droplets by nanoparticles can be adjusted by controlling the concentration of the nanoparticle suspension. The flow fields around the Janus droplets moving in a microchannel were observed with tracing particles. Finally, the electrokinetic velocity of the Janus droplets in a microchannel was measured. The effects of the strength of the electrical field, the surface coverage of the Janus droplets by nanoparticles, the size of the droplets as well as the electrolyte concentration on the electrokinetic velocity of the Janus droplets were studied.

Key Words: charged nanoparticles, electrokinetic motion, Janus droplet, microchannels, vortices

1. Introduction

Janus droplets comprised of two segments with different properties have attracted significant interest recently. Due to their specific properties, Janus droplets are suitable for the applications in many fields, such as biotechnology, materials science, pharmaceutical science, food analysis as well as chemistry. For example, Janus particles with color [1], electrical [2], magnetic [3, 4] and amphiphilic [5] anisotropies made from Janus droplets can be used for stabilizing emulsion[6], fabricating twisting-ball electronic paper [7], detecting biomolecular [8, 9] and so on. Janus droplets also have potential in drug delivery with the advantages of carrying multiple substances and delivering them to specific sites[10–12].

The means for generating Janus droplets have been developed and presented in some papers, which can be grossly divided into two groups: high energy mixing method [13–20] and microfluidic method [7, 8, 10, 21–42]. The high energy mixing method can prepare Janus emulsions simply and quickly, and includes the following two steps: a) add two immiscible dispersed phases, usually oils, into a continuous phase, usually an aqueous solution; b) vibrate the mixture using a shear mixer or a vortexer until the emulsion appears homogeneous. The surface heterogeneity of the Janus droplets generated with this method is dependent on both the three interfacial tensions and the volume ratios of the three phases. For example, Ge et al. [15] generated vegetable oil-silicon oil Janus droplets in Tween 80 aqueous solution. They found that the topology of the droplets could be adjusted by changing the surfactant concentration or the volume ratio of the two immiscible dispersed phases. By adding hexane and perfluorohexane into an aqueous solution with Zonyl and sodium dodecyl sulfate (SDS) as surfactants, Zarzar et al. [16] fabricated hexane-perfluorohexane Janus droplets. Their experimental results indicate that Janus droplets with different topologies can be formed by varying the ratio between SDS

and Zonyl. Compared with other ways, this high energy mixing method has the advantage of being able to prepare a large number of Janus droplets within limited time. Recently, the droplet microfluidic system has been developed and widely used for generating and manipulating droplets [43–45], which provides a potential way to form Janus droplets. Based on the formation mechanism, the microfluidic method can be divided into three groups: breakup formation [7, 8, 21–28], evolution from core-shell emulsion [10, 29–33] and phase separation [34–36]. The first mechanism, breakup formation, is the most popular one. With this mechanism, Janus droplets can be produced one by one by forcing parallel streams of two immiscible phases to break up into droplets in a T-shape microchannel [22]. Maeda et al. [23] extended this method by developing a centrifuge Janus droplet generator to synthesis magnetic anisotropic Janus droplets. The synthesis system comprises two parts: a droplet generator device with built-in capillaries for holding the two immiscible monomers and forming sessile Janus droplets on the capillary orifices, a tabletop centrifuge which is used to provide centrifugal force to drag the sessile Janus droplets away and form mobile Janus droplets. Furthermore, to increase the volume throughput of the microfluidic method, a lot of attempts have been taken, for example, parallelization devices were utilized to generate multiple Janus droplets at the same time [37–42].

Apart from the two methods, some other methods were also developed to make Janus droplets. Bormashenko et al. [46] produced a Janus droplet by merging one droplet coated with carbon black powder with another droplet coated with polytetrafluoroethylene powder. The Janus droplets partially covered with polydopamine (PDA) particles and hydroxide ions (OH^-) were fabricated by Xu et al. [47] based on the mechanism that the particles and ions occupy separate areas on oil droplets. Rozynek and his colleagues [48] generated Janus droplets with two hemispheres coated with different particles in a leaky dielectric liquid. Under externally applied

electric field, electrohydrodynamic (EHD) flow is generated around oil droplets coated with different particles, which drives the particles on the droplets to move and form “ribbon-like” structures, and then Janus droplet can be prepared by merging the droplets. In one of our previous published papers [49], a sessile Janus droplet was produced by partially covering the oil droplet with aluminum oxide (Al_2O_3) nanoparticles under applied electrical field. As oil-water interface and aluminum oxide nanoparticles carry opposite signs of charges, this sessile droplet is electrically anisotropic. Although various methods have been developed to form Janus droplets, very few methods are reported for generating mobile electrically anisotropic Janus droplets. For example, the existing microfluidic method fabricates Janus droplets by breaking up two immiscible organic liquid phases into droplets, and the two sides of the droplets carry surface charges of the same sign when contacting with aqueous solution. However, each of the electrically anisotropic Janus droplets presented in this paper has one side with positive surface charge and another side with negative surface charge. These Janus droplets have potential applications in electronic paper, controlling flow in microchannels, delivering drugs and so on.

Due to anisotropic properties, many electrokinetic phenomena of Janus particles and Janus droplets are unique, and have attracted significant interest recently. Peng et al. [50] studied the AC electroosmosis in vicinity an immobile metal-dielectric sphere. They found that vortices could always form around the Janus sphere regardless the electric field was vertical or parallel to the plane between its two hemispheres (conductive hemisphere and dielectric hemisphere). The electrophoretic motion of Janus particles has been theoretically and experimentally studied in some papers [51–55]. Squires et al. [55] theoretically studied the electrophoresis of metallodielectric Janus particle and found that the Janus particle trended to move towards its dielectric side under alternating current (AC) electric field because of the induced-charge

electroosmotic flow on the metallic side. Then Gangwal et al. [54] experimentally proved this finding by observing the electrophoresis of metal-dielectric Janus particles, which were formed by partially covering the polystyrene particles with gold. The motion of metallodielectric Janus particles in a microchannel under externally applied direct current (DC) electrical field has been studied in Daghighi's series papers [56–58]. Through numerical study, it has been found that the Janus particle in a microchannel moves faster than the dielectric particle or metal particle [56]. For the metallodielectric Janus particle with the dielectric hemisphere back to the electrical field, two large vortices form on one side of the Janus particle and act as engines to make the Janus particle move faster. Later, they [58] conducted experiments to measure the electrokinetic velocities of metal-dielectric Janus particles and dielectric particles of the same size in microchannels. They results indicate that the Janus particles moves much faster than the dielectric particles, which matches with the theoretical analysis. Apart from metallodielectric particles, Zhang et al. [59] studied the electrokinetic motion of Janus particles consisting of two hemispheres with different polarizabilities in a microchannel, and showed a possible way of separating Janus particles by size and the polarizability ratio between the two hemispheres of the Janus particles. Dielectrophoresis (DEP) is the motion of dielectric particles/droplets in non-uniform electrical fields [60], and some papers studied the DEP of Janus particles under AC electrical field [61–67]. For example, Honegger et al. [64] studied the rotation of Janus particles by DEP, and found that the rotation speed was related to the communication frequency. The DEP induced Janus particle assembly was experimentally studied by Zhang et al. [66], and they showed that the Janus particles got assembled when the medium conductivity was low and the assembly could be disrupted by increasing the medium conductivity. However, for the electrokinetic motion of electrically anisotropic Janus droplets, very few studies are reported and

the existing research is focused on the electroosmotic flow around sessile Janus droplets. In one of our previously published papers [68], the electroosmotic flow field around sessile dipolar Janus droplets was studied. The results indicate that vortices exist around the Janus droplet. The location and the size of the vortices are dependent on the topology of the droplet. The flow field and the electrokinetic motion of movable Janus droplets in microchannels are important in many applications such as micromixing, drug delivery, sorting and separation. So far, very little is known about this. Therefore, research in the flow field and the electrokinetic motion of movable Janus droplets in microchannels is highly desirable.

In this paper, we first reported a new method for preparing mobile electrically anisotropic Janus droplets with Al_2O_3 nanoparticle suspension in a microfluidic chip under DC electrical field. The effect of the Al_2O_3 nanoparticle concentration on the surface coverage of the Janus droplets by nanoparticles was studied. The flow fields in vicinity of Janus droplets were visualized when they moved in a microchannel under electrical field. Furthermore, the electrokinetic velocity of Janus droplets in a microchannel was measured. The effects of the strength of the electrical field, the surface coverage of the Janus droplets by nanoparticles, the droplet size as well as the electrolyte concentration on the electrokinetic velocities of Janus droplets were studied.

2. Materials and methods

2.1 Materials

Aluminum oxide passivated aluminum nanoparticles with the mean diameter of 18nm were provided by US Research Nanomaterials, Inc., USA. The thickness of the aluminum oxide shell wrapping the aluminum core was 2~5nm. Tween 20 (nonionic surfactant, impurities ≤ 3.0%) was purchased from Sigma-Aldrich which was used without further treatment. The oil was vegetable

oil (pure canola oil from Mazola Corporation) with the density of 918.7kg/m^3. Solid potassium chloride (KCl) of 99% purity was purchased from Sigma-Aldrich. Deionized water was obtained from a Milli-Q reagent water system. The resistance of the deionized water was 18.2MΩ•cm at 25℃.

2.2 Preparation of Pickering emulsion

Aluminum oxide nanoparticles and nonionic surfactant (Tween 20) were used as stabilizers to prepare oil-in-water Pickering emulsion. First, aluminum oxide nanoparticles were dispersed into deionized water using an ultrasonic cleaner (Cody Technology Limited Co., China) in the following way: a) Put certain amount of aluminum oxide nanoparticles into a glass bottle with a volume of 15mL (21mm (*d*) × 70mm (*h*)); b) Add deionized water (5mL) into the bottle followed by ultrasonic treatment for 8min. After the generation of nanoparticle suspension, put 100μL Tween 20 and 1mL oil into the bottle. Emulsification could be made by vibrating the mixture with a vortexer (VWR Scientific) at the speed of 3200rpm for 2min. The nonionic surfactant served as emulsifier to speed up emulsification and stabilize emulsion without changing the electrical property of the oil-water interface. As the zeta potential of aluminum oxide nanoparticles was positive from pH 2.5 to pH 8, they adhered on the negatively charged oil droplets automatically and Pickering emulsion formed finally (Figure 1 (a)). Let the emulsion stand for 48 hours, the extra nanoparticles in the water phase would sink to the bottom of the bottle and separate from the droplets by gravity. Figure 1 (b) shows the photograph of oil-in-water Pickering emulsion after standing for 48 hours. It's clearly shown in this figure that the droplets floating on the top layer are black due to the coverage of nanoparticles.

2.3 Formation of Janus droplets in a microchannel

In this study, the microfluidic chip was made by the soft lithograph method by bonding a polydimethylsiloxane (PDMS) layer with a microchannel on a glass substrate. Briefly, the master of the PDMS microstructure was fabricated first by coating the photoresist (SU-8 2075, MicroChem, USA) onto a silicon wafer. Then, a film carrying the pattern was placed on top of the wafer coated with a SU8 film after soft baking. And expose them to ultraviolet (UV) light. With the post exposure baking and the developing processes, a master with microchannel pattern on the silicon wafer was obtained. The mixture of PDMS and the curing agent (10:1 (w/w)) was poured on the master and heated at 80℃ for 1h. The PDMS layer with the microchannel structures was then peeled off carefully from the master and put into a plasma cleaner (HARRICK PLASMA, Ithaca, NY) with a glass slide for 1min. Finally, the microfluidic chip was assembled by placing the PDMS layer on the top of the glass slide. As shown in Figure 2(a), the microfluidic chip comprises a straight microchannel with a size of 1cm × 150μm × 80μm (length × width × height) for the formation and motion of Janus droplets and a confinement chamber with a size of 0.5cm × 1cm × 80μm (length × width × height) for holding droplets. An electrode insert port with the diameter of 1.5mm is set next to the joint between the confinement chamber and the microchannel for placing electrode. The effect of the droplets in the confinement chamber on the electrical field can be eliminated by inserting the electrode into this port rather than into the inlet well. Another electrode is inserted in the outlet well.

After the microfluidic chip was fabricated, 10μL buffer solution was added into the outlet well first to wet the microchannel. Then 5μL emulsion was added into the inlet well and the droplets would flow into the droplet confinement chamber. Due to the limitation of the height of the confinement chamber, only those droplets with the diameter smaller than 80μm could enter it.

Afterwards, 100μL buffer solution was loaded into the inlet well and outlet well, respectively. The electrical field was applied to the microchannel with a DC power supply (CSI12001X, Circuit Specialist Inc., USA) via two platinum electrodes inserted in the electrode insert port and outlet well, respectively. Under electrical field, the oil droplets entered the microchannel from the confinement chamber and moved through it. At the same time, the positively charged Al_2O_3 nanoparticles adsorbed on the oil droplet were accumulated to one side of the oil droplet back to the electrical field. Janus droplets partially covered with Al_2O_3 nanoparticles could be formed in this way, as shown in Figure 2(b). The images of a droplet with uniformly covered Al_2O_3 nanoparticles before applying electrical field and a Janus droplet with Al_2O_3 nanoparticles covered on one side after applying the electric field are shown in Figure 3. As shown in Figure 3(a), the Al_2O_3 nanoparticles distribute uniformly on the oil droplet. After applying DC electrical field of 50V/cm from left to right, the positively charged nanoparticles move to the right-hand side of the droplet and a color and electrically anisotropic Janus droplet forms, as shown in Figure 3(b).

As the Janus droplets are formed from Pickering emulsion by electric field, the total number of Al_2O_3 nanoparticles adhering on the oil droplets affects the surface coverage of the Janus droplets by nanoparticles. The surface coverage of Janus droplets by nanoparticles (r) changes with the nanoparticle concentration (C) used for generating Pickering emulsion. To study the variation of r with C, four different concentrations of aluminum oxide nanoparticle suspensions, 0.5mg/mL, 1mg/mL, 1.5mg/mL and 2mg/mL, were used to generate Pickering emulsions and subsequently the Janus droplets, respectively.

2.4 Visualization of vortices

Spherical polystyrene particles of 1μm in diameter (Bangs Laboratories Inc., IN, USA) were employed as tracers to indicate the flow fields around Janus droplets. The experimental system, as shown in Figure 4, is composed of the microfluidic chip, a DC power supply, an optical microscope (Ti-E, Nikon) and imaging system. In the experiment, the microfluidic chip which held nanoparticle covered oil droplets was fixed on the microscope stage, and the liquid levels in the inlet and outlet wells were carefully balanced by injecting certain amount of tracing particle suspension with a digital pipette. Then apply electric field to the microchannel via two platinum electrodes inserted in the electrode insert port and the outlet well. Under this electrical field, Janus droplets formed quickly in the microchannel and the surface coverage (r) remained constant under the given electric field. The flow fields around Janus droplets were observed in the electrical field of 30V/cm. The images of the flow fields around Janus droplets were taken by a charge coupled device (CCD) camera (DS-Qi1Mc ,Nikon) assembled in the microscope, and were stored in a computer. Generally, the flow field changes with the variation of the topology of the Janus droplets. The flow fields around Janus droplets with different surface coverage generated with 1mg/mL and 2mg/mL nanoparticle suspension were observed, respectively.

2.5 Measurement of the droplets' velocity

The electrokinetic motions of oil droplets and Janus droplets were measured with the same experimental system as shown in Figure 4. The motions of oil droplets/Janus droplets were recorded by the CCD camera at the frame rate of 25fps under externally applied electrical field. The accuracy of this system in determining the position of droplets was approximately ±2 pixels corresponding to ±1.1μm. By measuring the travelling distance under certain time for an individual droplet with imaging analysis software, the velocity of the Janus droplet could be

obtained. Under each condition, 30 independent measurements were conducted. The experiments were carried out at room temperature (23-25℃).

Furthermore, to minimize the effect of hydrostatic pressure on the electrokinetic motion of Janus droplets, two measures were adopted: a) Large inlet and outlet wells were used to minimize the water level difference caused by electroosmotic flow in microchannel; b) After applying the electrical field for 30~40s, the electrical field was reverse to balance the water level of the wells.

3. Results and discussion

3.1 Formation of Janus droplets with different surface coverage by nanoparticles (*r*)

Figure 5 shows the variation of surface coverage of Janus droplets by Al_2O_3 nanoparticles, *r*, with the concentration of the nanoparticle suspension, *C*. The microscope image over each bar is the picture of Janus droplet generated with the corresponding nanoparticle suspension under electrical field of 50V/cm. It is seen in this figure that *r* increases with *C*. This phenomenon can be understood as follows. With other parameters unchanged, when high concentration of nanoparticle suspension is used to generate Pickering emulsion, the total number of nanoparticles adsorbed on the surface of oil droplets increases, which results in Janus droplets with a large surface coverage by nanoparticles under a given electric field. It should be noted that, as the nanoparticle coverage region of small Janus droplets cannot be seen clearly, only the Janus droplets with a diameter larger than 40μm were chosen to measure the surface coverage.

3.2 Vortices in vicinity of Janus droplet

Consider an oil droplet uniformly coated with Al_2O_3 nanoparticles. Under DC electrical field, the nanoparticles move to one side of the oil droplet facing the cathode of the electrical field, and

leave the other side as pure oil-water interface without the presence of nanoparticles. As the signs of surface charges of the oil-water interface and the Al_2O_3 nanoparticles are opposite, the electric double layer (EDL) field along the Janus droplet is dipolar. The interaction between the electrical field and the dipolar EDL generates electroosmotic flows with opposite directions on different segments of the Janus droplet. Consequently, vortices forms around the droplet.

In this study, the flow fields around two Janus droplets with the same size (the diameter d = 78μm) and different surface coverage (r = 40.6% and 21.1%) were examined. These two droplets were made with 2mg/mL nanoparticle suspension and 1mg/mL nanoparticle suspension, respectively. The flow fields around these Janus droplets under electrical field of 30V/cm are shown in Figure 6. It clearly indicates in Figure 6(a) that four vortices are generated around the mobile Janus droplet with r = 40.6% under the rightward electrical field. The two vortices are on the left side, while the other two stay on the right side. Figure 6(b) shows the flow field around the Janus droplet with smaller surface coverage by nanoparticles, r = 21.1%. As shown in this figure, under the same applied electrical field, only the two vortices on the right side of the Janus droplet exist, and the size of the vortices are smaller. With the decrease of the surface coverage of the Janus droplet, the electroosmotic flow on this side gets weaker and the electroosmotic flow on the other side becomes dominant; therefore, only the two vortices on the right side exist.

3.3 Electrokineitc motion of Janus droplet

3.3.1 Effects of the applied electrical field (E) and the surface coverage of nanoparticles (r)

The electrokinetic motion of a particle or a droplet in a microchannel is dependent on the combined effects of the electrophoretic motion of the particle or droplet and the electroosmotic

flow of the bulk solution in the channel. Therefore, the electrokinetic velocity of a droplet V_{ek} can be given as[69]:

$$V_{ek} = V_{eof} + V_{ep} \quad (1)$$

where V_{eof} is the electroosmotic flow velocity of the solution in the microchannel, V_{ep} is the electrophoresis velocity of the droplet. For a negatively charged oil droplet moving in a microchannel with negative zeta potential, V_{eof} is opposite to V_{ep}. Based on Eq. (1), we can easily find that, with V_{eof} fixed, the electrokientic velocity V_{ek} increases with the decrease of the electrophoresis velocity of the oil droplet V_{ep}. Moreover, V_{eof} and V_{ep} are linearly proportional to the externally applied electrical field which can be calculated through the following equations:

$$V_{eof} = \mu_{eof} \cdot E \quad (2)$$

$$V_{ep} = \mu_{ep} \cdot E \quad (3)$$

where μ_{eof} is the electroosmotic mobility and μ_{ep} is the electrophoresis mobility. Substituting Eq. (2) and (3) into Eq. (1), the expression of the electrokinetic velocity in terms of the strength of the electrical field can be written as:

$$V_{ek} = (\mu_{eof} + \mu_{ep}) \cdot E \quad (4)$$

Clearly, the electrokinetic velocity of droplets V_{ek} is linearly proportional to the electrical field, E.

It is well-known that for a negatively charged particle/droplet in a negatively charged microchannel, the electrophoretic motion of the particle/droplet is opposite to the electroosmotic flow in the channel. In other words, the electrokinetic velocity of the particle/droplet, V_{ek}, as

indicated by Eq. (1), is smaller than the electroosmotic flow velocity (V_{eof}) due to the electrophoretic motion of the particle/droplet. While the electroosmotic flow in microchannel is the same, the difference of the electrokinetic motion between an oil droplet and a Janus droplet of the same size is mainly caused by the different electrophoresis motions of the two droplets. Figure 7 shows the schematics of the electrophoresis of an oil droplet and a Janus droplet. As shown in Figure 7(a), for a negatively charged oil droplet, under externally applied electrical field, the electrical force acting on it $F_{e,o}$ can be given by:

$$F_{e,o} = QE \tag{5}$$

where Q is the total surface charge on the oil droplet. In the case of a Janus droplet, as shown in Figure 7(b), the electrical force $F_{e,J}$ can be calculated by:

$$F_{e,J} = F_{e,n} + F_{e,p} = (Q^- + Q^+)E \tag{6}$$

where $F_{e,n}$ is the electrical force on the left side, $F_{e,p}$ is the electrical force on the right side, Q^- and Q^+ are the total surface charge on the left and right sides, respectively. Compared with the oil droplet, the net surface charge on the Janus droplet is lower, because $Q_{net} = (Q^- + Q^+) = (Q^- - \lfloor Q^+ \rfloor)$. Therefore, the electrophoresis of the Janus droplet is slower than that of the oil droplet, which keeps decreasing with the increase of the positively charged area. Consequently, based on Eq. (1), the net velocity of the Janus droplet is higher than that of the pure oil droplet under the same condition. The same conclusion can be obtained by considering the hydrodynamic force acting on the droplets. As shown in Figure 7(a), under externally applied electrical field, from left to right, the electroosmotic flow can be generated on the negatively charged oil droplet, the direction of the electroosmotic flow is identical to that of the local electric field. The rightward electroosmotic flow on the droplet generates a hydrodynamic force

against the leftward electrophoretic force acting on the oil droplet. In the case of an electrically anisotropic Janus droplet, the directions of electroosmotic flow are opposite on different sides of the droplet, as shown in Figure 7(b). Correspondingly, these two electroosmotic flows generate opposite hydrodynamic forces. When the surface coverage of the positively charge nanoparticles increases and approaches to 40~50%, these two hydrodynamic forces approximately cancel each other. In the meantime, the net surface charge of the whole droplet and hence the electrophoresis is approaching to zero. Therefore, the net velocity of the Janus droplet in the microchannel increases with the surface coverage of the positively charged nanoparticles on the Janus droplet.

In order to verify this prediction, Janus oil droplets and pure oil droplets of 75μm±3μm in diameter were chosen in the experimental investigation. The electrokinetic velocities of Janus droplets with different surface coverage by aluminum oxide nanoparticles and oil droplets in terms of the electrical field are shown in Figure 8. Clearly, the velocity of Janus droplets is larger than the velocity of oil droplets under identical DC electrical field. And the larger the surface coverage of the Janus droplet by nanoparticles (r), the faster the electrokinetic motion in a microchannel. Furthermore, the results also indicate the effect of the electric field on the electrokinetic motion of oil droplets and Janus droplets. As shown in this figure, the velocities of oil droplets and Janus droplets increase with the applied DC electrical field linearly.

3.3.2 Effect of the Janus droplet size

The electrokinetic motion of Janus droplets in a microchannel can also be affected by the size of them. The electrokinetic velocities of Janus droplets with two different sizes, d = 75μm±3μm and d = 45μm±2μm were measured and compared. These droplets were generated with a nanoparticle suspension of C = 2mg/mL. As shown in Figure 9, under the same applied electrical

field, the larger Janus droplets move faster than the smaller ones. For a larger droplet, the gaps between the droplet and the channel walls are smaller. Consequently, the electrical lines are squeezed further in the smaller gap, and the electrical field is stronger in this region. The stronger electrical field in the smaller gaps will generate stronger electroosmotic flow, which promotes the motion of the Janus droplet. This phenomenon is called the "wall effect" and has been studied in some papers for electrokinetic transport of solid particles in microchannels [70], [71]. Generally, the smaller the size difference between a particle/droplet and a channel, the more significant the wall enhancing effect. Therefore, for a larger Janus droplet and a smaller Janus droplet moving in the same microchannel, the wall enhancing effect makes the larger Janus droplet move faster.

3.3.3 Effect of the electrolyte concentration

The effect of the electrolyte concentration on the electrokinetic velocity of Janus droplets was also investigated. The buffer solution used is 1mM KCl solution which was prepared by dissolving solid potassium chloride into deionized water. The electrokinetic velocities of Janus droplets in deionized water and 1mM KCl solution are shown in Table 1. By comparing the data shown in Table 1, it can be seen that the electrokinetic velocity decreases significantly when the buffer solution is changed from deionized water to 1mM KCl solution. For example, under applied electrical field of 50V/cm, the average electrokinetic velocity of the Janus droplets in deionized water is 183.2μm/s. However, in 1mM KCl solution, the average velocity decreases to 46.2μm/s.

The electroosmotic flow velocity V_{eof} in microchannels can be calculated by:

$$V_{eof} = -\frac{\varepsilon_o \varepsilon_r \zeta}{\mu} E \qquad (7)$$

where E is the applied electrical field, ε_o is the dielectric permittivity in vacuum, ε_r is the dielectric constant of the buffer solution, μ is the viscosity of the buffer solution and ζ is the zeta potential of the channel walls. It is well-known that the absolute value of zeta potential decreases when contacting with high-concentration buffer solution. For example, in deionized water, the zeta potential for PDMS microchannel is –60mV [72]. The zeta potential reduces to –20mV in 1mM KCl solution [73]. Therefore, under applied electrical field of 50V/cm, the electroosmotic flow velocities in a microchannel for deionized water and 1mM KCl solution can be calculated to be 236.1μm/s and 78.7μm/s, respectively. The comparison between the calculated electroosmotic flow velocities and the measured electrokinetic velocities of Janus droplets clearly shows that the reduction of the electrokinetic velocity of Janus droplets is mainly caused by the decrease of electroosmotic flow velocity in the microchannel.

Conclusion

A new method to fabricate mobile electrically anisotropic Janus droplets partially covered with Al_2O_3 nanoparticles in a microchannel under electrical field was presented in this paper. The surface coverage of the Janus droplets by nanoparticles can be controlled by adjusting the concentrations of Al_2O_3 nanoparticle suspensions. The Janus droplets with a large surface coverage by nanoparticles can be formed by using a high-concentration nanoparticle suspension. The electrokinetic flow fields around these Janus droplets were observed in this paper. The existence of the vortices in vicinity of a mobile Janus droplet in a microchannel under electrical field due to the opposite electroosmotic flow on different sides of the droplet was demonstrated. Furthermore, the electrokinetic velocities of the Janus droplets in a microchannel were measured. By comparing the electrokinetic velocities of Janus droplets under different conditions, the

following conclusions can be drawn: (a) The velocity of the Janus droplets increases with the strength of the electrical field and the surface coverage of the Janus droplets by nanoparticles; (b) If the surface coverage of the Janus droplets and the strength of the electrical field are the same, the larger Janus droplets move faster than the smaller ones due to the wall enhancing effect; (c) With the increase of the ionic concentration of the electrolyte solution, the electrokinetic velocity of the Janus droplets decreases due to the decreased zeta potential of the channel walls.

Acknowledgements

The authors appreciate the financial support of the Natural Sciences and Engineering Research Council (NSERC) of Canada through a research grant to D. Li.

References

[1] Nisisako, T., Torii, T., Higuchi, T., *Chem. Eng. J.* 2004, *101*, 23–29.

[2] Nisisako, T., Torii, T., Takahashi, T., Takizawa, Y., *Adv. Mater.* 2006, *18*, 1152–1156.

[3] Yu, X., Zhang, C., You, S., Liu, H., Zhang, L., Liu, W., Guo, S. S., Zhao, X. Z., *Appl. Phys. Lett.* 2016, *108*, 073504.

[4] Shepherd, R. F., Conrad, J. C., Rhodes, S. K., Link, D. R., Marquez, M., Weitz, D. A., Lewis, J. A., *Langmuir* 2006, *22*, 8618–8622.

[5] Xu, K., Ge, X. H., Huang, J. P., Dang, Z. X., Xu, J. H., Luo, G. S., *RSC Adv.* 2015, *5*, 46981–46988.

[6] Zhao, Y., Gu, H., Xie, Z., Shum, H. C., Wang B., Gu, Z., *J. Am. Chem. Soc.* 2013, *135*, 54–57.

[7] Khan, I. U., Serra, C. A., Anton, N., Li, X., Akasov, R., Messaddeq, N., Kraus, I., Vandamme,T. F., *Int. J. Pharm.* 2014, *473*, 239–249.

[8] Yang, Y. T., Wei, J., Li, X., Wu, L. J., Chang, Z. Q., Serra, C. A., *Adv. Powder Technol.* 2015, *26*, 156–162.

[9] Lan, J., Chen, J., Li, N., Ji, X., Yu, M., He, Z., *Talanta* 2016, *151*, 126–131.

[10] Shum, H. C., Zhao, Y. J., Kim, S. H., Weitz, D. A., *Angew. Chemie* 2011, *50*, 1648–1651.

[11] Laugel, C., Baillet, A., Youenang Piemi, M. P., Marty, J. P., Ferrier, D., *Int. J. Pharm.* 1998, *160*, 109–117.

[12] Zhao, C. X., *Adv. Drug Deliv. Rev.* 2013, *65*, 1420–1446.

[13] Zarzar, L. D., Sresht, V., Sletten, E. M., Kalow, J. A., Blankschtein D., Swager, T. M., *Nature* 2015, *518*, 520–524.

[14] Hasinovic, H., Friberg, S. E., *Langmuir* 2011, *27*, 6584–6588.

[15] Ge, L., Shao, W., Lu, S., Guo, R., *Soft Matter* 2014, *10*, 4498–4505.

[16] Hasinovic, H., Friberg, S. E., Rong, G., *J. Colloid Interface Sci.* 2011, *354*, 424–426.

[17] Yoon, J., Lee, K. J., Lahann, J., *J. Mater. Chem.* 2011, *21*, 8502–8510.

[18] Friberg, S. E., Kovach, I., Koetz, J., *ChemPhysChem* 2013, *14*, 3772–3776.

[19] Ge, L., Lu, S., Guo, R., *J. Colloid Interface Sci.* 2014, *423*, 108–112.

[20] Tu, F., Lee, D., *J. Am. Chem. Soc.* 2014, *136*, 9999–10006.

[21] Nisisako, T., Torii, T., *Adv. Mater.* 2007, *19*, 1489–1493.

[22] Nisisako, T., Hatsuzawa, T., *Microfluid. Nanofluid.* 2010, *9*, 427–437.

[23] Maeda, K., Onoe, H., Takinoue, M., Takeuchi, S., *Adv. Mater.* 2012, *24*, 1340–1346.

[24] Hirama, H., Odera, T., Torii, T., Moriguchi, H., *Biomed. Microdevices* 2012, *14*, 689–697.

[25] Zhang, M. Y., Zhao, H., Xu, J. H., Luo, G. S., *RSC Adv.* 2015, *5*, 32768–32774.

[26] Xu, K., Ge, X. H., Huang, J. P., Dang, Z. X., Xu, J. H., Luo, G. S., *RSC Adv.* 2015, *5*, 46981–46988.

[27] Nisisako, T., Hatsuzawa, T., *Sensors Actuators B: Chem.* 2016, *223*, 209–216.

[28] Ge, X., Huang, J., Xu, J., Chen, J., Luo, G., *Soft Matter* 2016, *12*, 3425–3430.

[29] Nie, Z., Xu, S., Seo, M., Lewis, P. C., Kumacheva, E., *J. Am. Chem. Soc.* 2005, *127*, 8058–8063.

[30] Utada, A. S., Lorenceau, E., Link, D. R., Kaplan, P. D., Stone, H. A., Weitz, D. A., *Science* 2005, *308*, 537–541.

[31] Nisisako, T., Okushima, S., Torii, T., *Soft Matter* 2005, *1*, 23-27.

[32] Hayward, R. C., Utada, A. S., Dan, N., Weitz, D. A., *Langmuir* 2006, *22*, 4457–4461.

[33] Pannacci, N., Bruus, H., Bartolo, D., Etchart, I., Lockhart, T., Hennequin, Y., Willaime, H., Tabeling, P., *Phys. Rev. Lett.* 2008, *101*, 164502.

[34] Choi, C. H., Weitz, D. A., Lee, C. S., *Adv. Mater.* 2013, *25*, 2536–2541.

[35] Jeong, J., Gross, A., Wei, W. S., Tu, F., Lee, D., Collings, P. J., Yodh, A. G., *Soft Matter* 2015, *11*, 6747–6754.

[36] Zhang, Q., Xu, M., Liu, X., Zhao, W., Zong, C., Yu, Y., Wang, Q., Gai, H., *Chem. Commun.* 2016, *52*, 5015–5018.

[37] Nisisako, T., Ando, T., Hatsuzawa, T., *Lab Chip* 2012, *12*, 3426-3435.

[38] Muluneh, M., Issadore, D., *Lab Chip* 2013, *13*, 4750–4754.

[39] Conchouso, D., Castro, D., Khan, S. A., Foulds, I. G., *Lab Chip* 2014, *14*, 3011–3020.

[40] Femmer, T., Jans, A., Eswein, R., Anwar, N., Moeller, M., Wessling, M., Kuehne, A. J., *ACS Appl. Mater. Interfaces* 2015, *7*, 12635–12638.

[41] Jeong, H. H., Yelleswarapu, V. R., Yadavali, S., Issadore, D., Lee, D., *Lab Chip* 2015, *15*, 4387–4392.

[42] Nisisako, T., *Curr. Opin. Colloid Interface Sci.* 2016, *25*, 1–12.

[43] Ahn, M. M., Im, D. J., Yoo, B. S., Kang, I. S., *Electrophoresis* 2015, *36*, 2086–2093.

[44] Joensson, H. N., Zhang, C., Uhlén, M., Andersson-Svahn, H., *Electrophoresis* 2012, *33*, 436–439.

[45] Schoeman, R. M., Kemna, E. W., Wolbers, F., Berg, A., *Electrophoresis* 2014, *35*, 385–392.

[46] Bormashenko, E., Bormashenko, Y., Pogreb, R., Gendelman, O., *Langmuir* 2011, *27*, 7–10.

[47] Xu, J., Ma, A., Liu, T., Lu, C., Wang, D., Xu, H., *Chem. Commun.* 2013, *49*, 10871–10873.

[48] Rozynek, Z., Mikkelsen, A., Dommersnes, P., Fossum, J. O., *Nat. Commun.* 2014, *5*, 1–6.

[49] Li, M., Li, D., *J. Nanoparticle Res.* 2016, *18*, 1-14.

[50] Peng, C., Lazo, I., Shiyanovskii, S. V., Lavrentovich, O. D., *Phys. Rev. E* 2014, *90*, 051002.

[51] Hsu, J. P., Huang, H. T., Yeh, L. H., Tseng, S., *Langmuir* 2012, *28*, 2997–3004.

[52] Boymelgreen, A. M., Miloh, T., *Phys. Fluids* 2012, *24*, 870-879.

[53] Boymelgreen, A. M., Miloh, T., *Phys. Fluids* 2011, *23*, 072007.

[54] Gangwal, S., Cayre, O. J., Bazant, M. Z., Velev, O. D., *Phys. Rev. Lett.* 2008, *100*, 058302.

[55] Squires, T. M., Bazant, M. Z., *J. Fluid Mech.* 2006, *560*, 65–101.

[56] Daghighi, Y., Gao, Y., Li, D., *Electrochim. Acta* 2011, *56*, 4254–4262.

[57] Daghighi, Y., Li, D., *Lab Chip* 2011, *11*, 2929–2940.

[58] Daghighi, Y., Sinn, I., Kopelman, R., Li, D., *Electrochim. Acta* 2013, *87*, 270–276.

[59] Zhang, F., Li, D., *J. Colloid Interface Sci.* 2015, *448*, 297–305.

[60] Zeinali, S., Çetin, B., Oliaei, S. N., Karpat, Y., *Electrophoresis* 2015, *36*, 1432–1442.

[61] Boymelgreen, A., Yossifon, G., Park, S., Miloh, T., *Phys. Rev. E* 2014, *89*, 011003.

[62] Zhang, L., Zhu, Y., *Langmuir* 2012, *28*, 13201–13207.

[63] García-Sánchez, P., Ren, Y., Arcenegui, J. J., Morgan, H., Ramos, A., *Langmuir* 2012, *28*, 13861–13870.

[64] Honegger, T., Lecarme, O., Berton, K., Peyrade, D., *Microelectron. Eng.* 2010, *87*, 756–759.

[65] Zhang, L., Zhu, Y., *Appl. Phys. Lett.* 2010, *96*, 141902.

[66] Gangwal, S., Pawar, A., Kretzschmar, I., Velev, O. D., *Soft Matter* 2010, *6*, 1413-1418.

[67] Velev, O. D., Gangwal, S., Petsev, D. N., *Annual Reports Section "C" (Physical Chemistry)* 2009, *105*, 213–245.

[68] Li, M., Li, D., *Microfluid. Nanofluid.* 2016, *20*, 79.

[69] Wuzhang, J., Song, Y., Sun, R., Pan, X., Li, D., *Electrophoresis* 2015, *36*, 2489–2497.

[70] Xuan, X., Ye, C., Li, D., *J. Colloid Interface Sci.* 2005, *289*, 286–290.

[71] Ye, C., Xuan, X., Li, D., *Microfluid. Nanofluid.* 2005, *1*, 234–241.

[72] Lee, G. B., Lin, C. H., Lee, K. H., Lin, Y. F., *Electrophoresis* 2005, *26*, 4616–4624.

[73] Chun, M. S., Shim, M. S., Choi, N. W., *Lab Chip* 2006, *6*, 302–309.

Table 1

The average values of the measured electrokinetic velocity of Janus droplets generated with nanoparticle suspension of C = 2 mg/mL under different electric field. (A) in deionized water; (B) in 1mM KCl solution. The diameter of the Janus droplets is d = 75 μm±3μm.

(A)						
Electric field (V/cm)	50	60	70	80	90	100
Electrokinetic velocity (μm/s)	183.2	227.8	270.8	297.2	338.8	375.0
Standard deviation	11.8	13.1	12.5	13.8	13.8	16.3
(B)						
Electric field (V/cm)	50	60	70	80	90	100
Electrokinetic velocity (μm/s)	46.2	55.2	66.0	75.0	79.3	88.8
Standard deviation	4.6	6.1	7.9	9.2	8.8	9.3

Figure Legends

Figure 1. (a) Schematic of the oil droplets with the nanoparticles adhering on the oil droplets; (b) A photograph of the Pickering emulsion obtained by mixing the Al_2O_3 nanoparticle suspension with oil and Tween 20.

Figure 2. (a) Schematic of the structure of the microfluidic chip; (b) Schematic of the generation of Janus droplets under applied DC electrical field.

Figure 3. Microscope images of (a) a droplet with uniformly covered Al_2O_3 nanoparticles before applying the electrical field and (b) a Janus droplet with Al_2O_3 nanoparticles covered on the right hand side under applied electrical field of 50V/cm. The nanoparticle concentration is C = 1mg/mL.

Figure 4. Schematic of the experimental system.

Figure 5. The variation of the surface coverage of Janus droplets by nanoparticles (r) with the concentration of the nanoparticle suspension (C). The microscope images over each bar are the pictures of Janus droplets generated with the corresponding nanoparticle suspensions under 50V/cm electrical field.

Figure 6. Vortices are generated around Janus droplets moving in a microchannel under externally applied DC electrical field of 30V/cm. (a) d = 78μm, r = 40.6%, generated with 2mg/mL nanoparticle suspension; (b) d = 78μm, r = 21.1%, generated with 1mg/mL nanoparticle suspension. The exposure time of the microscope is 400ms.

Figure 7. Schematics of the electrophoresis of (a) an oil droplet and (b) a Janus droplet.

Figure 8. The electrokinetic velocities of the Janus droplets generated with different concentrations of nanoparticle suspensions and oil droplets as a function of electrical field. The diameter of different types of droplets d is 75μm±3μm.

Figure 9. The electrokinetic velocity of Janus droplets with a diameter of 75μm±3μm and 45μm±2μm generated with nanoparticle suspension of C = 2mg/mL as a function of applied DC electrical field.

Figure 1

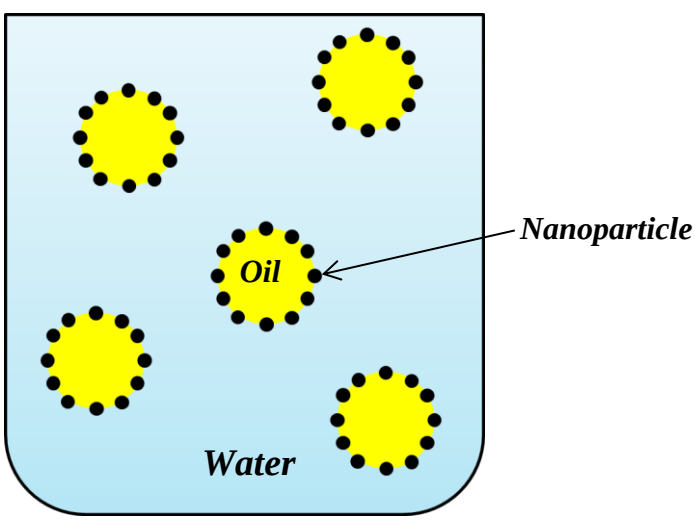

(a)

(b)

Figure 2

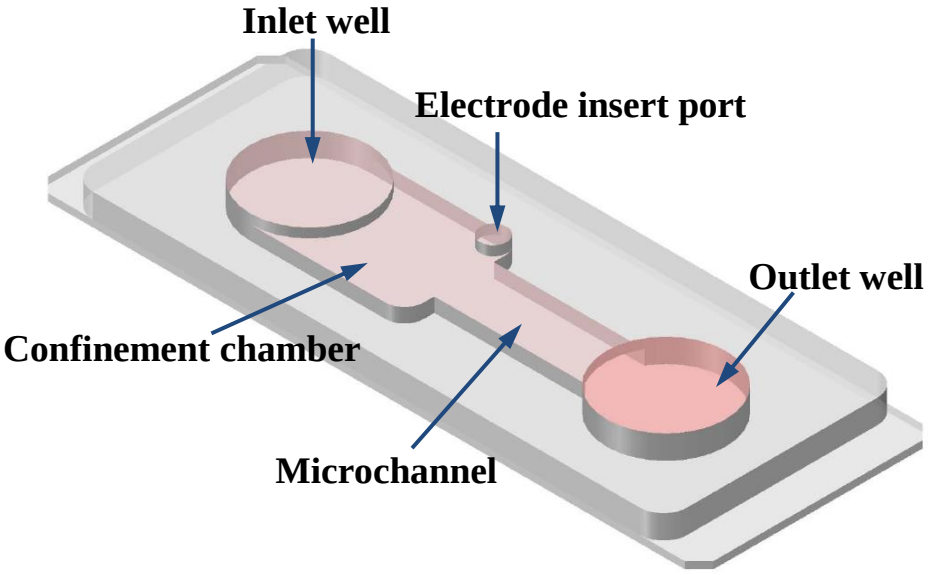
Inlet well
Electrode insert port
Outlet well
Confinement chamber
Microchannel

(a)

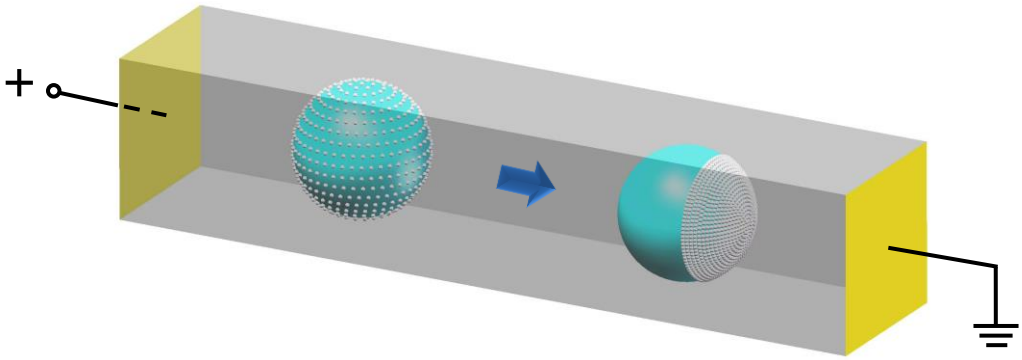
+

(b)

Figure 3

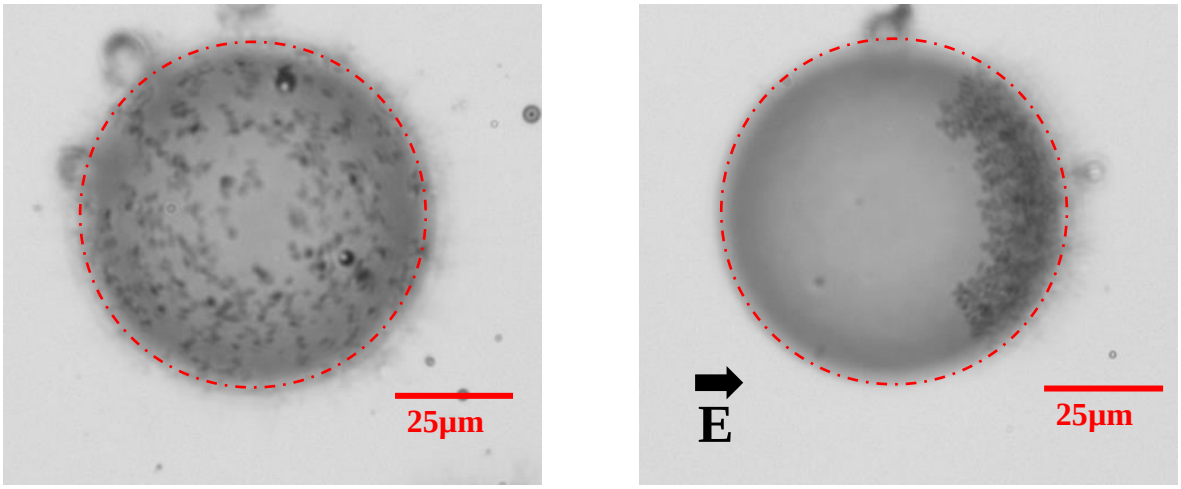

(a) (b)

Figure 4

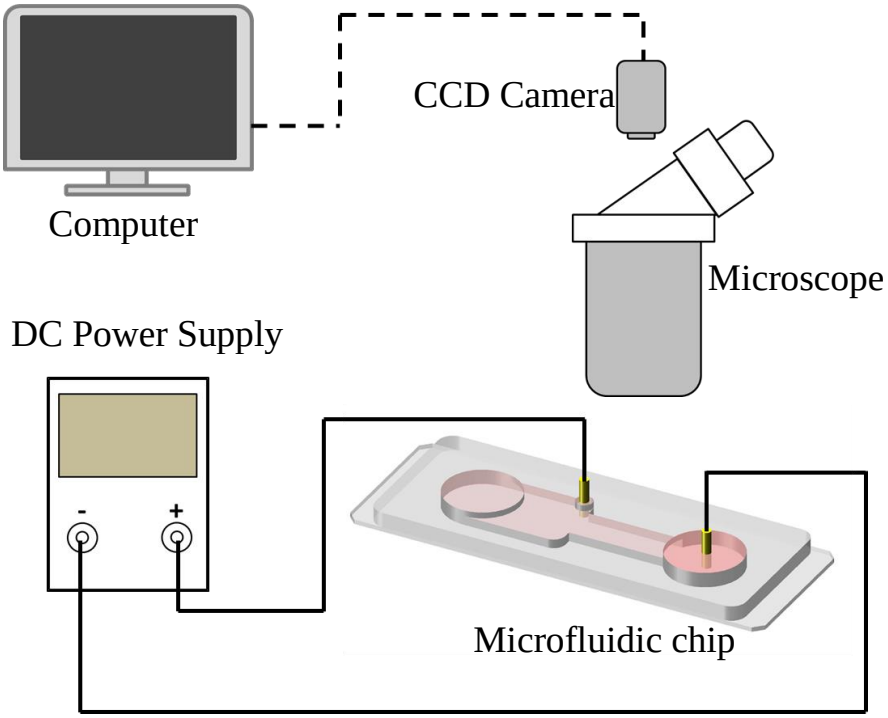
CCD Camera
Computer
Microscope
DC Power Supply
-
+
Microfluidic chip

Figure 5

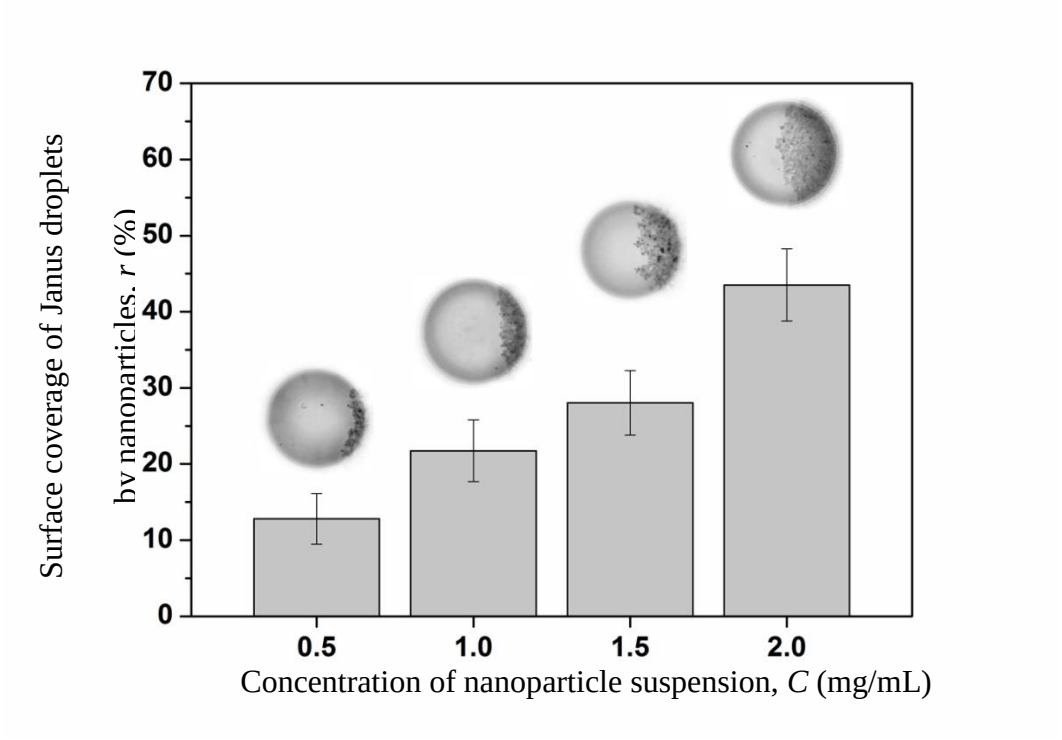
Surface coverage of Janus droplets
by nanoparticles, r (%)
70
60
50
40
30
20
10
0
0.5
1.0
1.5
2.0
Concentration of nanoparticle suspension, C (mg/mL)

Figure 6

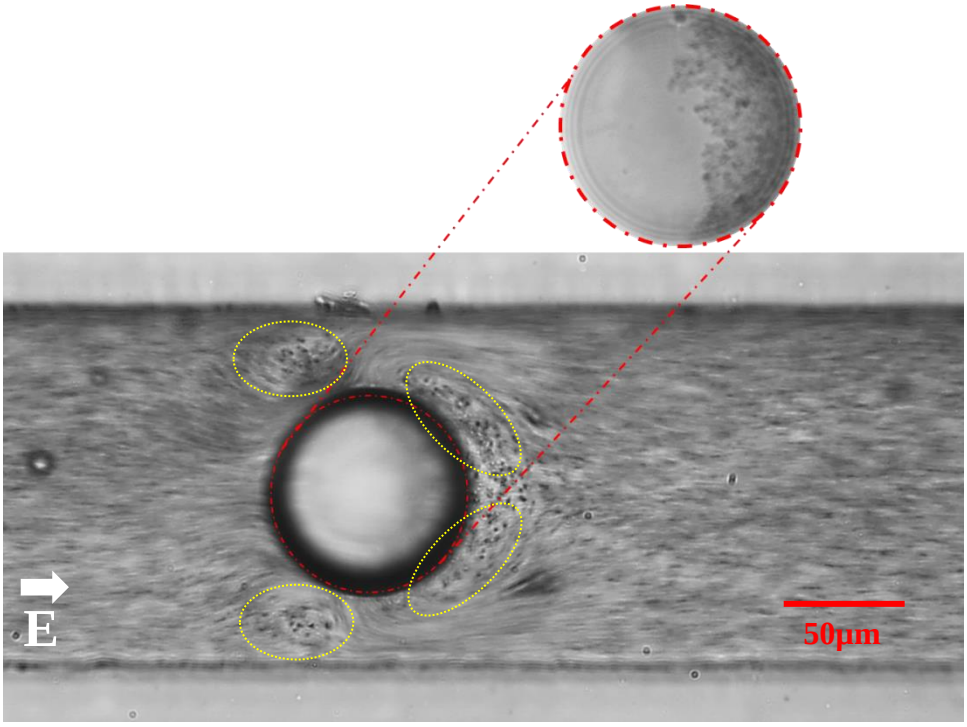

(a)

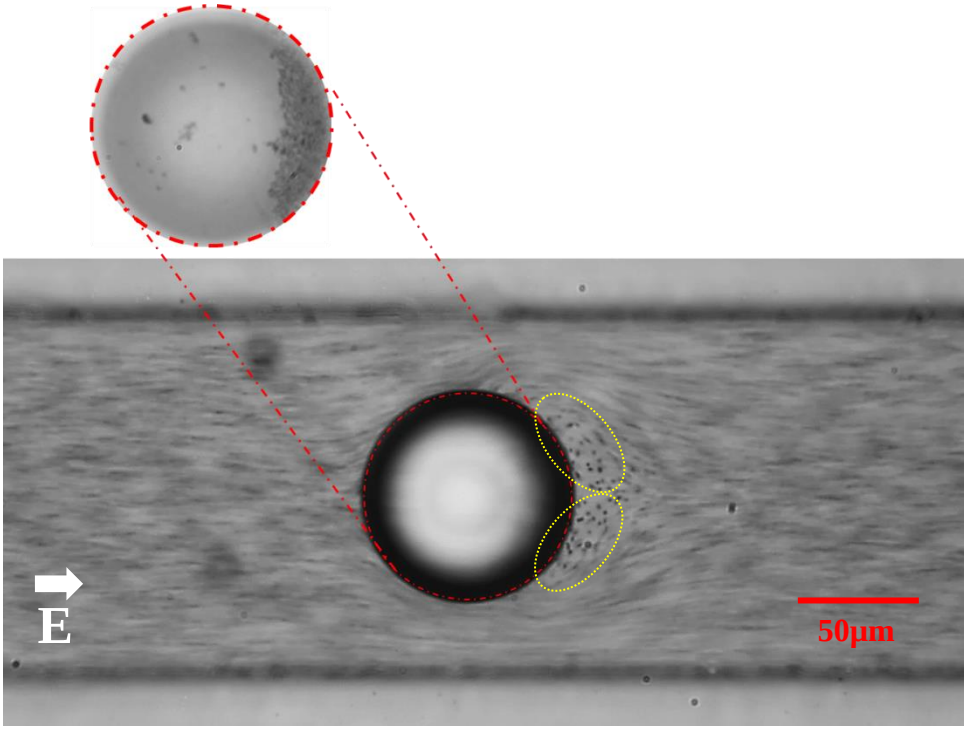

(b)

Figure 7

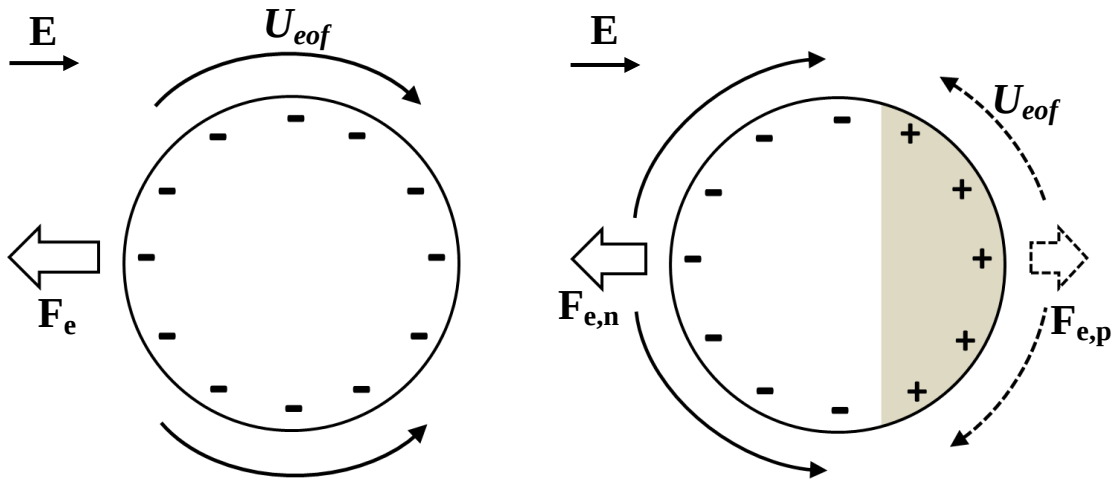

(a) (b)

Figure 8

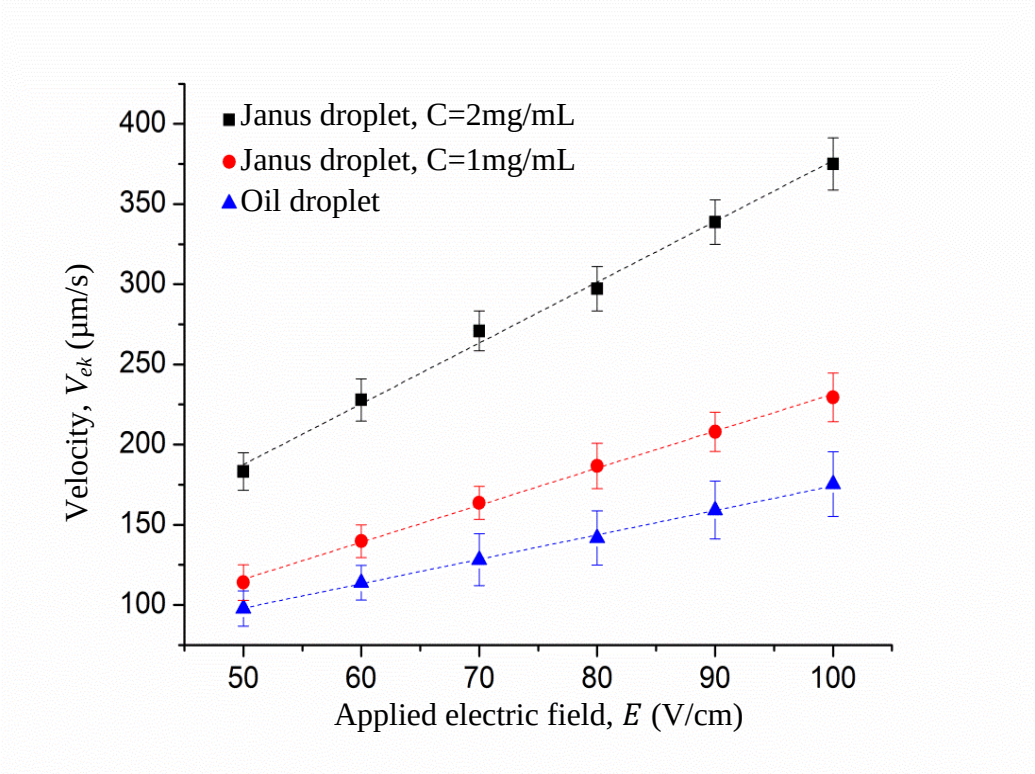
Janus droplet, C=2mg/mL
Janus droplet, C=1mg/mL
Oil droplet
Velocity, V_{ek} (μm/s)
400
350
300
250
200
150
100
50
60
70
80
90
100
Applied electric field, E (V/cm)

Figure 9

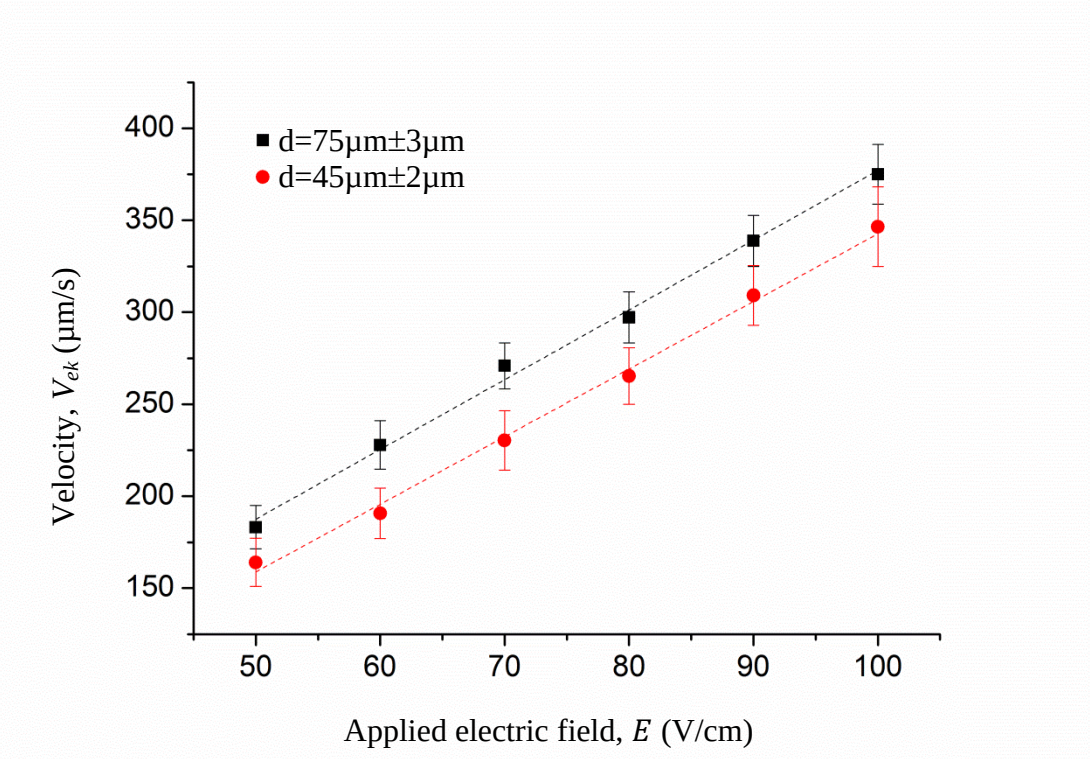
d=75μm±3μm
d=45μm±2μm
Velocity, V_{ek} (μm/s)
Applied electric field, E (V/cm)
400
350
300
250
200
150
50
60
70
80
90
100